*Journal of Modern Optics*
Vol. 53, Nos. 1–2, 10–20 January 2006, 87–96

Taylor & Francis
Taylor & Francis Group

# Control of high-order harmonic emission using attosecond pulse trains

J. BIEGERT*†, A. HEINRICH†, C. P. HAURI†, W. KORNELIS†,
P. SCHLUP†, M. P. ANSCOMBE†, M. B. GAARDE‡,
K. J. SCHAFER‡ and U. KELLER†

†ETH Zurich, Physics Department, 8093 Zurich, Switzerland
‡Louisiana State University, Physics Department, Baton Rouge, LA, USA

(*Received 2 March 2005; in final form 4 May 2005*)

We show that attosecond pulse trains are a natural tool to control strong field processes such as high-order harmonic generation. Coherently combining an attosecond pulse train with an IR driving field, we predict and experimentally confirm enhancement and spectral narrowing of the harmonic yield at photon energies around 90 eV. The use of an attosecond pulse train to seed the harmonic generation process replaces tunneling ionization with a single-photon ionization step, therefore permitting the manipulation of the time–frequency properties of high-order harmonic generation already at the single-atom level.

## 1. Introduction

The rapid advancement in laser physics [1, 2] allows scientists to study the elementary motion of atoms [3], probe the rotational and vibrational behaviour of molecules, and leads to a better understanding of complex biological systems. With high-order harmonic generation (HHG) [4, 5], which is a coherent up-conversion process extending the laser wavelength, typically in the near-infrared range, to the water window and beyond [6, 7], a table-top soft-X-ray (XUV) laser source is available which holds tremendous promise [8, 9] to make the XUV region more approachable. The real promise lies, however, in the possibility to generate attosecond pulses [10–12] from such a source, since the electron dynamics in atoms [13], which in turn governs any chemical reaction, occurs on the timescale of attoseconds. Attosecond pulse trains (APT) [14] and single attosecond pulses [15] have been generated, and a first demonstration experiment has shown the applicability of a single attosecond pulse to time-resolve an inner-shell decay in krypton [15]. Even though this source holds tremendous promise, a major drawback is its inefficiency and the lack of sufficient control over its properties, including over the spectral resolution or spectral position at a certain wavelength range. Record photon yields at 90 eV are around $10^8$ photons per laser shot [16] (compared to $10^{17}$ photons in an

*Corresponding author. Email: biegert@phys.ethz.ch

*Journal of Modern Optics*
ISSN 0950–0340 print/ISSN 1362–3044 online © 2006 Taylor & Francis
http://www.tandf.co.uk/journals
DOI: 10.1080/09500340500167669

IR pulse from a TW class laser), which are about two to four orders of magnitude below the requirements for XUV microscopy [17].

Many investigations of harmonic generation have been conducted with an eye towards optimizing different aspects of the process [18–22], and much has been learned about the dependence of the XUV emission on macroscopic parameters such as pump laser intensity, gas density, focusing conditions, and pump pulse length. Practically speaking, however, most attempts at optimization are frustrated by the highly nonlinear dependence of the process on the pump laser intensity when ionization is initiated by tunneling. Recent theoretical studies have shown, however, that enhancement and even control over electron wavepacket dynamics is nevertheless feasible on the single-atom level [23, 24] and even macroscopically [25], leading to an enhancement by at least two orders of magnitude. This is possible through a combination of an APT with an infrared (IR) field: the APT allows one to set the time of ionization, initial kinetic energy and emission direction of the electron wavepacket and thereby removes the disadvantages of strong field tunneling. The linear dependence of ionization on the strength of the APT leads to a large volume effect [25] since even atoms in the radial wings of the IR pulse contribute significantly to HHG, where in the tunneling case the intensity would be below threshold.

We present results from a first experiment showing the feasibility of enhancement of high-order harmonic generation, as a consequence of control over electron wavepacket dynamics in strong fields.

## 2. Theory

We have numerically solved [25] the macroscopic response of an ensemble of helium atoms by solving the three-dimensional Maxwell wave equation (MWE) in the slowly evolving wave approximation [2, 26]. The source terms for individual atoms were obtained from solutions to the time-dependent Schrödinger equation (TDSE) in the strong-field approximation [27]. The driving field at the entrance to the medium comprises the sum of a 27 fs IR pulse with a peak intensity of $5\times 10^{14}\,\mathrm{W/cm^2}$, and an APT, synthesized from the odd harmonics 11 through 19 of the IR pulse, whose envelope is taken as the fourth power of the IR field, with a peak intensity of $10^{13}\,\mathrm{W/cm^2}$. Both fields are described as Gaussian beams with maximum volume overlap such that the APT focus is kept at the centre of the medium and that both beam waists are similar over at least 1 mm of the medium. Figure 1 shows results calculated over a 1 mm long volume of helium atoms with a density of $2\times 10^{18}\,\mathrm{cm^{-3}}$. The lower curve in figure 1 shows the medium response when only the IR field ($5\times 10^{14}\,\mathrm{W/cm^2}$) is present. Adding the APT with an intensity of $10^{13}\,\mathrm{W/cm^2}$ results in a significant increase in harmonic signal by several orders of magnitude in the plateau region, with decreasing enhancement for increasing harmonic order. The enhancement shows a weak dependence, in the cutoff region, on the relative delay between IR pulse and APT (dashed, solid lines in figure 1). The TDSE simulations revealed a critical dependence of the single-atom harmonic emission spectrum strength and shape on the relative delay [24]. With the APT present, the harmonics are clearly resolved but with increasing spectral width with

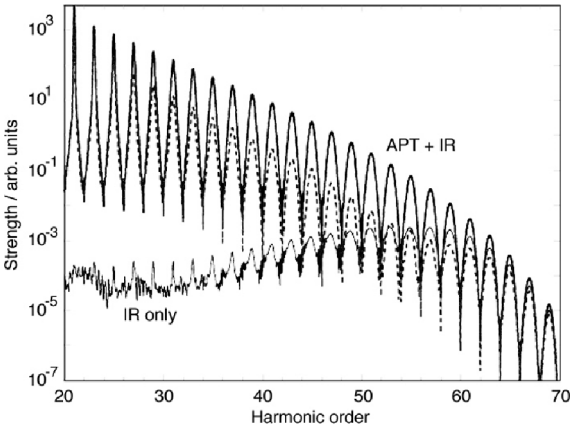


Figure 1. Harmonic spectra generated in helium: the lower curve is calculated with only the IR field for an intensity of $5 \times 10^{14}$ W/cm$^2$. The upper two curves show the medium response, with an additional APT (intensity of $10^{13}$ W/cm$^2$) for two different time delays of $-0.095$ IR cycles (solid line) and $+0.185$ IR cycles (dashed line).

harmonic order; a strong indication that the short quantum path dominates [24]. A detailed investigation [25] shows that the single-atom enhancement is stronger for low IR intensities compared to high intensities, so that atoms in the wings of the IR beam contribute nearly as strongly to the macroscopic enhancement as the atoms in the centre, leading to a large volume effect.

## 3. Experiment

### 3.1 *Setup*

The laser system is based on a commercial Ti:sapphire oscillator (Femtolasers) with two home-built amplifiers, one of which is cryogenically cooled, routinely delivering 27 fs pulses with an energy of up to 1 mJ at 1 kHz [28]. The experimental setup is shown in figure 2: 700 μJ of energy are focused with a silver-coated, spherical mirror, with a radius of curvature of 1500 mm, into a 50 mm long capillary with an inner diameter of 800 microns. The capillary is inside a vacuum chamber, filled with xenon. The backing pressure of xenon is varied between 0 and 25 mbar and differential pumping into the next vacuum chamber leads to a negative pressure gradient in the direction of propagation. Using a capillary serves three purposes: it improves phase matching [29, 30], reduces the gas flux into the chamber compared to a pinhole of the same size, thereby helping to keep the ambient pressure in the following chamber at a lower value, and acts as an extended spatial filter. The last point is important, since short quantum path selection is a prerequisite to yield regularly spaced pulses within the APT [14, 31]. We determined the intensity in the capillary to be $9.8 \times 10^{13}$ W/cm$^2$, sufficient to generate harmonics to the 19th order in xenon as required by the simulation. The emerging APT co-propagates inside the

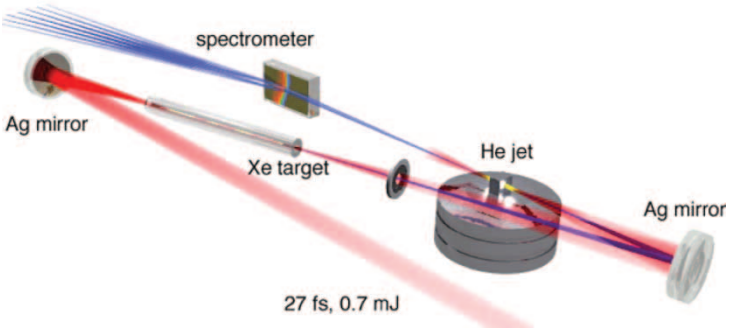


Figure 2. Setup of the experiment: 27 fs, 0.7 mJ pulses at a centre wavelength of 785 nm and at a repetition rate of 1 kHz are focused by a silver mirror into a 50 mm long and 800 micron diameter capillary, filled with xenon. The capillary is differentially pumped towards the exit port. The low-order harmonics propagate together with the leftover IR pulse to another silver mirror, which focuses the radiation into a pulsed helium target. The emerging high-order harmonics impinge into the entrance slit of a commercial XUV spectrometer. The spectra are recorded with a CCD with a fiber-coupled multi-channel plate. (The colour version of this figure is included in the online version of the journal.)

second vacuum chamber, to a second silver-coated spherical mirror with a radius of curvature of 300 mm. Both the IR and APT are focussed by this silver mirror into the helium target. By extrapolating measured values using the numerical package XOP [32], we estimate the reflectivity at a photon energy of 20 eV to be 5%. The helium target is a combination of a jet, pulsing at 1 kHz and which is synchronized with the laser, and a 2 mm long tube target to increase the interaction length [33]. Overall backing pressures for the helium target varied between 1400 mbar and 3000 mbar with the ambient pressure always being below $10^{-2}$ mbar in the chamber.

Without xenon present, the IR intensity was adjusted so as to yield a cutoff in helium around the 69th harmonic. From the cutoff, we estimate the IR intensity to be $4.6 \times 10^{14}$ W/cm$^2$. The generated harmonics propagate through a 1 mm diameter pinhole, which serves as pumping aperture, into another vacuum chamber with a typical ambient pressure of $10^{-6}$ mbar and finally into a XUV spectrometer (McPherson), which can be read out at the full repetition rate of the laser.

### 3.2 *Low-order harmonics control high-order harmonics*

Figure 3 shows results from a xenon pressure scan for constant helium pressure. First, we evacuated the capillary and, with no xenon present, no low-order harmonics are generated so the APT cannot be synthesized. The IR field is strong enough to generate very-high-order harmonics up to the 77th order in helium, as shown in figure 3(*a*). Next, we fill the capillary with xenon at 5 mbar and, as a consequence, low-order harmonics are generated, as shown in figure 3(*b*), and at the same time, the highest orders are significantly enhanced as predicted by our theory. Further increasing the xenon pressure to 15 mbar (figure 3(*c*)), we see strong harmonics for orders 11–19, and a further increase in the enhancement of the highest orders. Increasing the pressure further to 25 mbar (figure 3(*d*)), generation of

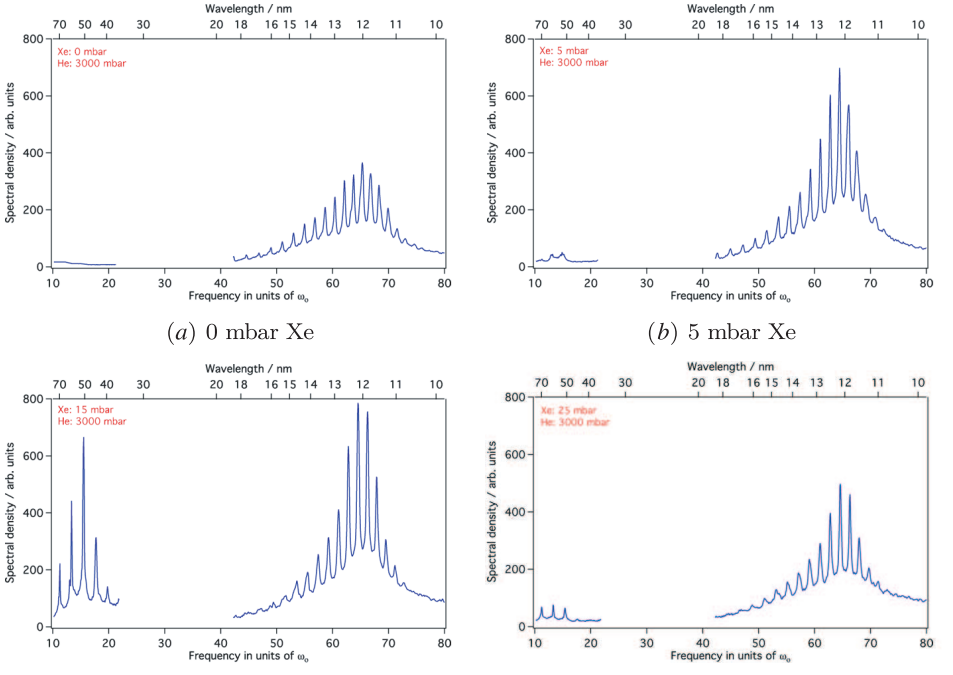


Figure 3. Measured harmonic spectra for identical pressures of helium for four distinct pressures in xenon. (*a*) Without xenon, no APT is generated and shown are the very-high-order harmonics generated in helium solely by the strong IR field. (*b*) With xenon at 5 mbar, the presence of the APT clearly influences the harmonics at the very highest orders. (*c*) With xenon at 15 mbar, we clearly see that the orders 11 to 19 are generated and the highest orders are enhanced further. (*d*) With xenon at 25 mbar, the re-absorption of the low orders inside the capillary decreases the APT strength and therefore the highest orders are diminished as well. (The colour version of this figure is included in the online version of the journal.)

low-order harmonics is decreased. We attribute the decrease to re-absorption [19] of the low orders inside the capillary since the high xenon pressure reduces the absorption length significantly below the capillary length. As a direct consequence, the enhancement of the highest orders is also diminished.

Figure 4 confirms the results shown in figure 3: shown are highest-order harmonics, between orders 45 and 75, generated only by the APT, the IR field alone, and by a combination of IR and APT. Since the APT is synthesized out of low-order harmonics 11 to 19 from xenon, the lowest trace (labeled only APT) does not exhibit any harmonic spectrum at the shown wavelength range. Furthermore, due to the saturation intensities of xenon, such high orders would be impossible to generate from xenon atoms. Without xenon, no APT is present, but, as described above, the IR field is strong enough to generate highest-order harmonics in helium alone, as shown by the curve labeled 'only IR'. Combining IR field and APT results in the uppermost curve, labeled APT + IR, which exhibits an enhancement in amplitude by a factor of 5 over the only IR case. Two more features are clearly

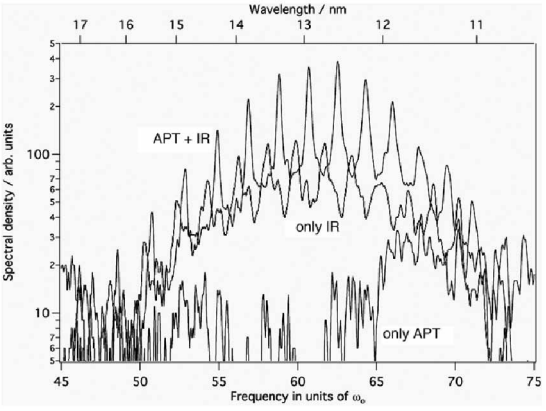


Figure 4. Measured highest-order harmonics for three cases: 'only APT', only xenon and no helium is present and the generated harmonics (11 to 19) synthesizing the APT are too low order to be visible in the graph. Furthermore, due to the low saturation intensity for xenon atoms, it is impossible to generate such high orders in xenon atoms; 'only IR', no xenon and, consequently, no APT is present. The IR field is, however, strong enough to generate highest-order harmonics in helium; 'APTs + IR', a clear enhancement in amplitude is observed.

present in figure 4: with APT and IR field present, the harmonics are blue-shifted, and their spectral widths are smaller compared to the 'only IR' case. The blue shift arises from the propagation of the IR field through an ionized medium in the capillary, which causes a significant blue shift [34, 35]. We estimated the blue shift from ADK theory [36] and it is in qualitative agreement with the observed values. Since the IR field, which is the determining factor for the photon energy gain of the high-order harmonics, is blue-shifted, the resulting harmonics are blue-shifted as well. The improved spectral resolution and reduced bandwidth is attributed to the fact that only the short quantum path contributes to harmonic generation.

### 3.3 *Dependence on pressure in xenon and helium*

Figures 5 and 6 show high harmonics between orders 45 and 75 for either varying helium (figure 5) or xenon (figure 6) while keeping the other pressure constant.

With the xenon pressure constant at 0 mbar and 15 mbar, we change the helium backing pressure for the gas jet from 1400 mbar to 3000 mbar. Figure 5(*a*) and (*b*) clearly show that the spectral positions of the harmonic peaks are fixed when the helium pressure is changed and that the cutoff moves to higher orders with increasing helium pressure. The increase in harmonic strength (amplitude) with increasing pressure is also a clear indication that the process was not saturated. The jet backing pressure of 3000 mbar was limited by the pumping capability of our setup. Figure 6(*a*) and (*b*) show the same spectral range for orders 45 to 75 with the helium pressure fixed at 1400 mbar and 3000 mbar and for varying xenon pressure. Figure 6(*a*) shows that, for increasing xenon pressure in the capillary, higher orders are more pronounced, and similar to the results in figure 3(*a*)–(*d*), if the pressure is too high, the enhancement decreases. With helium at 3000 mbar (figure 6(*b*)), we

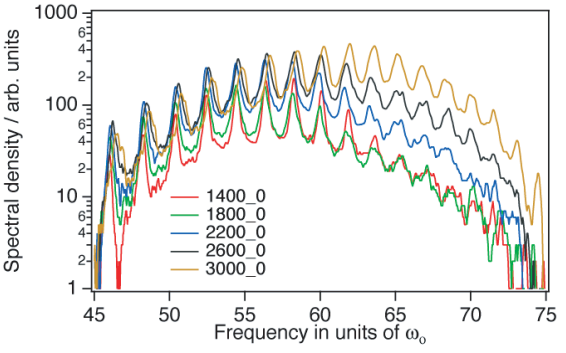


(*a*) Xe at 0 mbar

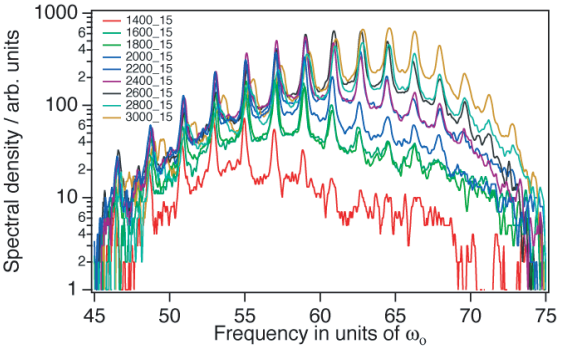


(*b*) Xe at 15 mbar

Figure 5. Measured harmonic spectra for varying pressures of helium for two distinct pressures in xenon. (*a*) No xenon: the graph shows high-order harmonics generated in helium by the IR field alone. (*b*) Xenon at 15 mbar: increasing the helium pressure increases the harmonic yield and shifts the cutoff to higher order. The harmonic peaks are, however, invariant as a function of pressure. (The colour version of this figure is included in the online version of the journal.)

observe much stronger harmonics with a cutoff shifted to higher energies. Similar to figure 4, we also observe a clear blue shift of the harmonic frequencies shown in figure 6 compared to figure 5.

We summarize our results from the pressure scans in figure 7: we estimated the spectral position of the highest harmonic yield by fitting an envelope function over the harmonic spectrum for orders 41 to 79. The loci of fitted peaks for varying xenon and helium pressures are calculated by interpolating between measured pressure values. Figure 7 shows that, with increasing helium pressure, the position of the envelope maximum shifts significantly, from order 54 to 61 with a pressure increase from 1800 to 3000 mbar, to higher photon energy. The spectral shift dependence on variation of xenon pressure is much less pronounced. This is advantageous if the source has to be tuned to a XUV laser wavelength and scaled in photon yield by using the above-mentioned volume effect.

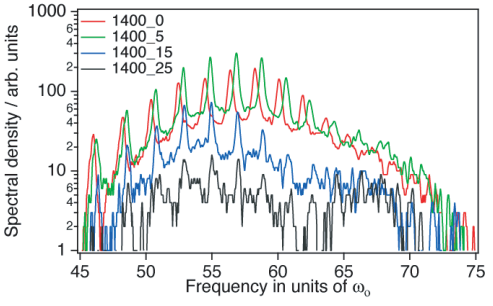


(*a*) He at 1400 mbar

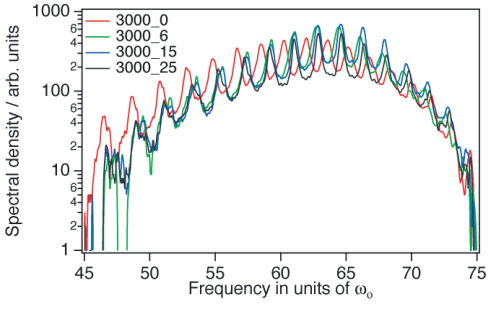


(*b*) He at 3000 mbar

Figure 6. Measured harmonic spectra for varying pressures of xenon for two distinct pressures in helium. (*a*) Helium at 1400 mbar: the graph shows high-order harmonics generated in helium by the IR field alone. (*b*) Helium at 3000 mbar: increasing the helium pressure increases the harmonic yield and shifts the cutoff to higher order. A clear blue shift of the harmonic peaks can be observed as a function of xenon pressure. (The colour version of this figure is included in the online version of the journal.)

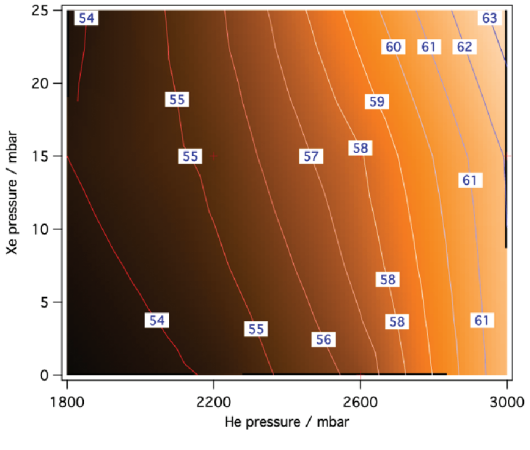


Figure 7. Fitting an envelope function over harmonic orders 41 to 79, the graph shows the position of the envelope maximum, in units of harmonic order, for varying xenon and helium pressures. (The colour version of this figure is included in the online version of the journal.)

## 4. Conclusions

Enhancement of high-order harmonic generation was observed by combining an APT with a driving IR field; first experimental results qualitatively confirm our earlier theoretical predictions [24, 25]. This would indicate that APTs are ideally suited to influencing the harmonic yield at a single atom level. The enhancement is retained by the macroscopic medium response as confirmed by our experimental results.

This not only shows that APTs are natural tools to influence harmonic generation on a single atom level, an effect not only persisting, but even smoothing out the macroscopic medium response thereby positively contributing to an increase in harmonic yield. Decoupling the ionization from the recombination steps allows one to tailor the spectral and spatial properties as well as the enhancement. We are convinced that large improvements over the demonstrated results are possible by choosing an improved interaction geometry, optimum time delay, and interaction volumes, which should increase photon yields such that they might reach the levels necessary even for XUV microscopy.

## Acknowledgements

This work was supported by the Swiss National Science Foundation (QP-NCCR) and by ETH Zurich. We acknowledge the support of EU FP 6 program 'Structuring the European Research Area', Marie Curie Research Training Network XTRA (contract No. FP6-505138).

## References

[1] G. Steinmeyer, D.H. Sutter, L. Gallmann, *et al.*, Science **286** 1507 (1999).
[2] T. Brabec and F. Krausz, Rev. Mod. Phys. **72** 545 (2000).
[3] A.H. Zewail, Science **242** 1645 (1988).
[4] J.J. Macklin, J.D. Kmetec and C.L. Gordon III, Phys. Rev. Lett. **70** 766 (1993).
[5] A. L'Huillier, M. Lewenstein, P. Salieres, *et al.*, Phys. Rev. A **48** R3433 (1993).
[6] E.A. Gibson, A. Paul, N. Wagner, *et al.*, Science **302** 95 (2003).
[7] J. Seres, E. Seres, A.J. Verhoef, *et al.*, Nature **433** 596 (2005).
[8] A. L'Huillier, T. Auguste, Ph. Balcou, *et al.*, J. Nonlin. Opt. Phys. Mat. **4** 647 (1995).
[9] G.A. Reider, J. Phys. D **37** R37 (2004).
[10] Gy. Farkas and Cs. Toth, Phys. Lett. A **168** 447 (1992).
[11] P. Antoine, A. L'Huillier and M. Lewenstein, Phys. Rev. Lett. **77** 1234 (1996).
[12] P. Agostini and L.F. DiMauro, Rep. Prog. Phys. **67** 813 (2004).
[13] A. Scrinzi, M. Geissler and T. Brabec, Laser Phys. **11** 169 (2001).
[14] P.M. Paul, E.S. Toma, P. Breger, *et al.*, Science **292** 1689 (2001).
[15] M. Drescher, M. Hentschel, R. Kienberger, *et al.*, Science **291** 1923 (2001).
[16] E. Takahashi, Y. Nabekawa and K. Midorikawa, RIKEN Rev. **49** 14 (2002).
[17] J.-C. Gauthier and A. Rousse, J. Phys. IV **12** 59 (2002).
[18] J. Zhou, J. Peatross, M.M. Murnane, *et al.*, Phys. Rev. Lett. **76** 752 (1996).
[19] M. Schnurer, Z. Cheng, M. Hentschel, *et al.*, Phys. Rev. Lett. **83** 722 (1999).
[20] E. Constant, E. Mevel, D. Garzella, *et al.*, J. Phys. **10** 35 (2000).

[21] I.J. Kim, H.T. Kim, C.M. Kim, *et al.*, Appl. Phys. B **78** 859 (2004).
[22] D.H. Reitze, S. Kazamias, F. Weihe, *et al.*, Opt. Lett. **29** 86 (2004).
[23] A.D. Bandrauk and N.H. Shon, Phys. Rev. A **66** 031401 (2002).
[24] K.J. Schafer, M.B. Gaarde, A. Heinrich, *et al.*, Phys. Rev. Lett. **92** 023003 (2004).
[25] M.B. Gaarde, K.J. Schafer, A. Heinrich, *et al.*, Phys. Rev. A (in press).
[26] E. Priori, G. Cerullo, M. Nisoli, *et al.*, Phys. Rev. A **6106** (2000).
[27] M. Lewenstein, Ph. Balcou, M.Yu. Ivanov, *et al.*, Phys. Rev. A **49** 2117 (1994).
[28] W. Kornelis, M. Bruck, F.W. Helbing, *et al.*, Appl. Phys. B **79** 1033 (2004).
[29] C.G. Durfee, A.R. Rundquist, S. Backus, *et al.*, Phys. Rev. Lett. **83** 2187 (1999).
[30] I.P. Christov, H.C. Kapteyn and M.M. Murnane, Opt. Exp. **7** 362 (2000).
[31] Y. Mairesse, A. de Bohan, L.J. Frasinski, *et al.*, Science **302** 1540 (2003).
[32] http://www.esrf.fr/computing/scientific/xop.
[33] A. Heinrich, M. Bruck, C.P. Hauri, *et al.*, Gas target for efficient high harmonic generation. CLEO/QELS, San Francisco, CA (2004).
[34] E. Yablonovitch, Phys. Rev. Lett. **60** 795 (1988).
[35] C. Altucci, R. Bruzzese, C. de Lisio, *et al.*, Phys. Rev. A **61** 021801 (2000).
[36] M.V. Ammosov, N.B. Delone and V.P. Krainov, Soviet Phys. JETP **64** 1191 (1986).